

A Rotation Face to Face Through-hole Wireless Power Transfer System

Liangyu Bai, Jianquan Zhang, Yanmin Liu

Key Laboratory of Space Utilization, Technology and Engineering Center for space Utilization, Chinese Academy of Sciences

ABSTRACT

Contactless slip-ring provide a safe, non-contact, high efficiency, wear-free and reliable power transfer solution with low maintenance for rotary applications. In this paper, a novel magnetic coupler of wireless power transfer (WPT) system is designed. Compared with the traditional slip ring power supply, it can be applied to the rotating condition. To realize light-weight and small-volume of the WPT, the magnetic coupler and circuit have been optimized from both compensation topology and coil configuration. Experimental results are demonstrating that transfer power is 280W at efficiency of 91.7%.

Keywords: wireless power transfer, rotary magnetic coupler, reluctance model, through-hole

1. INTRODUCTION

Removing the cable between a power source and a load is very important in many applications, e.g., for a plug-in electric vehicle battery charger, or a slip ring in space applications, the power cable is the restriction factor for reliability and maintenance performance. Thus, wireless power transfer (WPT) with air gaps high output power and high efficiency is a very important technology.

Due to a large winding separation, the WPT system has relatively large leakage inductance and reduced magnetizing flux. Compensation for loose coupling can be achieved through the use of resonance circuits which enable the boosting of voltage or current in the secondary to usable levels.

The researchers have performed a great deal of work on WPT systems, unfortunately, these studies have low level of integration, they take up a lot of space.

This study has focused on a general design that system has smaller volume, higher integration. The equivalent coupling circuit based on a mutual inductance model is described in Section 2. In Section 3 the

optimization method of magnetic model is proposed. Section 4 validates and analyses the modified model from WPT system. Finally, the conclusions of the study are given.

2. THEORETICAL ANALYSIS AND SYSTEM STRUCTURE

2.1 Theoretical Analysis

Poor transmission efficiency not only shortens the life span of the WPT system, but also could cause severe heating effect, the transmission efficiency becomes a very important issue for the application. To reduce system weight and temperature rise, core losses should be eliminated. The most desirable way to minimize the core losses is to maximize efficiency.

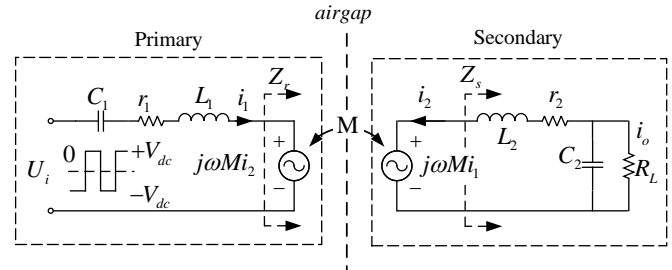


Fig 1 Mutual inductance coupling model of the WPT system

Due to the high operating frequency, the skin effect is terrible. Litz wires are commonly considered to have lower ac resistances than solid wires. Not only the skin effect but also proximity effect is drastically reduced. In this study air core coils with litz wire are used for the primary and secondary coils. The mutual inductance coupling model of the WPT system is shown in Figure 2.

The transmission efficiency can be derived as:

$$\eta = \frac{R_L I_o^2}{r_1 I_1^2 + r_2 I_2^2 + R_L I_o^2} \quad (1)$$

Theoretically, the system is operated at the secondary resonant frequency, which is determined by:

$$\omega_0 = \frac{1}{\sqrt{C_2 L_2}} \quad (2)$$

Then, the system transmission efficiency can be simplified as:

$$\eta = \frac{R_L}{r_2 + R_L + \frac{r_1 r_2^2}{\omega_0^2 M^2} + \frac{r_1 L_2^2}{M^2} + \frac{r_3 R_L^2 C_2}{L_2} + \frac{2r_1 r_2 R_L}{\omega_0^2 M^2} + \frac{r_1 r_2^2 R_L^2 C_2^2}{M^2}} \quad (3)$$

$$\cong \frac{R_L}{r_2 + R_L + \frac{r_1 r_2^2}{\omega_0^2 k^2 L_1 L_2} + \frac{r_1 L_2}{k^2 L_1} + \frac{r_2 R_L^2}{\omega_0^2 L_2^2}}$$

2.2 Magnetic Model

The winding differs regarding their leakage flux distribution. To associate the geometry of the rotating transformer with its electrical behavior, the reluctance model is built for each winding arrangement. The

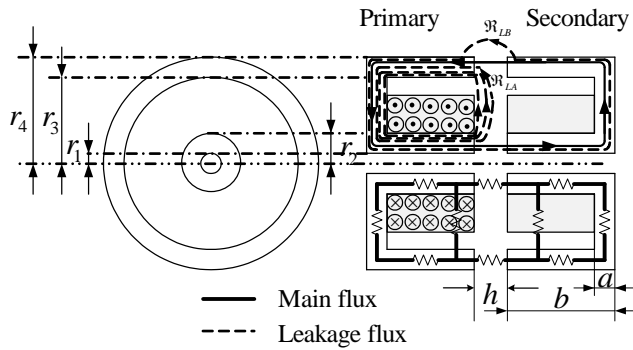


Fig 2 Cross sectional area of core transformer

reluctance model is converted to an electric model. A cut of the rotating transformer with coaxial windings is presented in Figure 2.

There are two magnetic flux sources and two windings N_1 (primary winding) and N_2 (secondary winding) that are conducting currents i_1 and i_2 respectively. The flux paths in the magnetic core and the air space are shown with

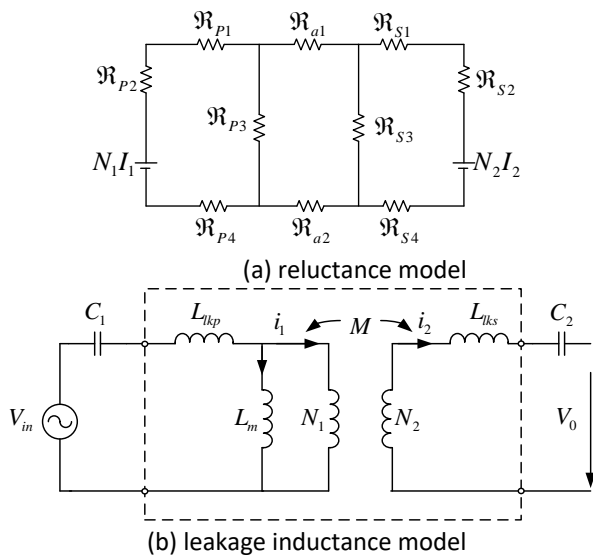


Fig 3 Transformation from reluctance model to leakage inductance model

dashed lines. The equivalent magnetic reluctance model and circuit model appears in Figure 3.

In Figure 3, between reluctance model and circuit model, it can be shown as

$$L_m = \frac{N_1 N_2}{\sum \mathfrak{R}_m} \quad (4)$$

$$L_{lk} = \frac{\mu_0 \pi (b-a)(r_3 + r_2) N^2}{r_3 - r_2} \quad (5)$$

From equation (5), the leakage expression of the magnetic circuit is not related to the distance between primary coil and secondary coil, which is inconsistent with the facts and cannot be describing the leakage well. Therefore, the magnetic model should be improved.

2.3 Influence of Coil Distance

Firstly, the internal resistance of the primary coil and the secondary coil is assumed as 0.1Ω to simplify the analysis in simulation. The inverter is modeled as a constant current source (Fig.1), the operating frequency is 20kHz. The distance of the coils is selected in the range of 4mm to 20mm. The coils distance range is assumed to be 4mm, 8mm, 12mm, 16mm and 20mm, respectively. The load is adopted as 10Ω , the turns of the coil is assumed to be same, so $n=1=N_1/N_2$, N_1 and N_2 are primary and secondary coil turns respectively. The voltage gain to the coils distance variations of system are shown in Fig. 4.

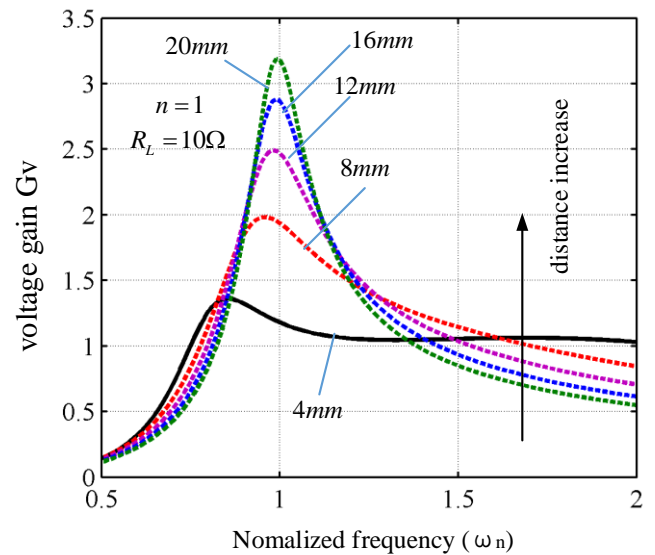


Fig 4 The curve of transfer characteristics when distance of the coils varied

It is known from Fig.4 that the voltage gain $G_v = U_0/U_i$ is increased with the increase of distance, but the increasing trend of the G_v becomes slower as the distance becomes larger.

2.4 Modified Magnetic Model

According to the Figure 2, each part of magnetic flux is divided into the magnetic flux tube which is easy to calculate the magnetic resistance, and corresponds to the magnetic circuit model[2][3]. Figure 5 shows the schematic diagram of the section of magnetic flux tube in the magnetic core window and the equivalent semi-elliptical flux tube. Leakage flux through the magnetic core window is show in Figure 5(a). Figure 2 \mathfrak{R}_{LA} corresponds to a magnetic flux tube section approximately half ellipse, and the long axis is l_1 , and short axis is $2h$. Figure 5(b) is the equivalent semi-elliptical flux tube structure and corresponding size.

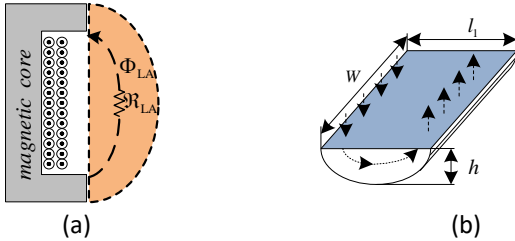


Fig 5 Sketch of Flux tubes partitioning in magnetic core windows

The corresponding magnetic resistance is the function of the air gap, it can be shown as

$$\mathfrak{R}_{LA}(h) = \frac{\pi[1.5(120h^{0.4} - 4.9 + h) - \sqrt{h(120h^{0.4} - 4.9)}]}{\mu_0 W(240h^{0.4} - 9.8 + 2h)} \quad (6)$$

Figure 6 shows the sketch of flux tubes partitioning in magnetic core columns. The leakage flux Φ_{LB} through the magnetic resistance \mathfrak{R}_{LB} is shown in Figure 6(a). The corresponding magnetic flux tube section \mathfrak{R}_{LB} is approximately half cylinder, and figure 6(b) is the equivalent semi-elliptical flux structure and corresponding size. Magnetic resistance is a function of the distance between the original side and the magnetic core:

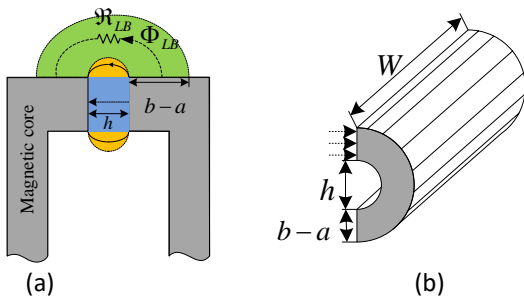


Fig 6 Sketch of Flux tubes partitioning in magnetic core side columns

$$\mathfrak{R}_{LB}(h) = \frac{1.27\pi(\frac{h}{b-a} + 1)}{\mu_0 W} \quad (7)$$

The improved magnetic circuit model can be obtained by using the above subdivision flux tube. The proposed core is made of UF cores(UF25D).

Existing model (Figure 3 (a)), the core window area approximate equivalent to the \mathfrak{R}_{P3} , consider only through the window of the circle magnetic flux tube \mathfrak{R}_{LA} , and ignores half elliptical magnetic resistance of magnetic flux tube, also did not consider the core side column area of leakage flux \mathfrak{R}_{LB} , and for \mathfrak{R}_{P3} has nothing to do with the distance, the measured and theoretical analysis, the magnetic flux leakage is related to the air gap, the original method to calculate the loosely coupled transformer magnetic flux leakage can cause larger error.

Tab. 1 Reluctances of the transformer model

Magnetic resistance	value
$\mathfrak{R}_{P1}, \mathfrak{R}_{S1}$	$b / (\mu_0 \mu_r \pi (r_4^2 - r_3^2))$
$\mathfrak{R}_{P2}, \mathfrak{R}_{S2}$	$(r_3 - r_2) / (\mu_0 \mu_r \pi a (r_3 + r_2))$
$\mathfrak{R}_{P3}, \mathfrak{R}_{S3}$	$(r_3 - r_2) / (\mu_0 \pi (b - a) (r_2 + r_3))$
$\mathfrak{R}_{P4}, \mathfrak{R}_{S4}$	$b / (\mu_0 \mu_r \pi (r_2^2 - r_1^2))$
\mathfrak{R}_{a1}	$h / (\mu_0 \pi (r_2^2 - r_1^2))$
\mathfrak{R}_{a2}	$h / (\mu_0 \pi (r_4^2 - r_3^2))$
\mathfrak{R}_{LA}	equation(6)
\mathfrak{R}_{LB}	equation(7)

In order to verify the modified magnetic circuit model, it can be shown in Figure 7, the calculated value of the primary inductance from the existing model is far less than that of the measured value, and the error is

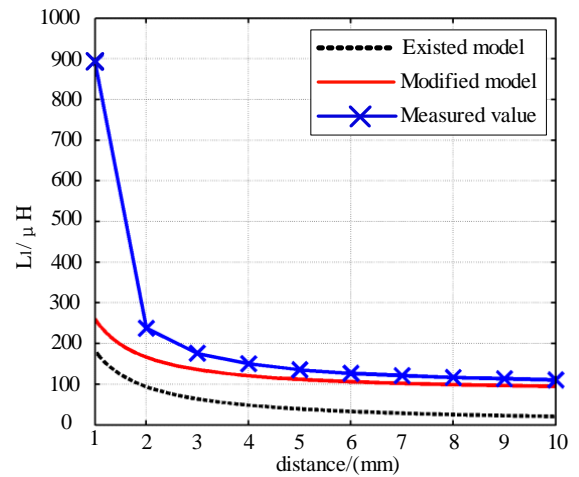


Fig 7 Comparison between reluctance models

large, the calculated value of the modified value is closer to the measured value.

3. EXPERIMENTAL EVALUATION

To verify the theoretical analysis and the design criteria, the laboratory level experimental setup is built. From Figure 8 it can be seen that a new through-hole type contactless slipring with identical primary and secondary magnetic structures proposed. As it can be seen the face to face configuration of this system allows for flexible air gaps. One of the clear advantages of this structure is that it accommodates the possibility of linear and rotary movement for the secondary as compared to the existing coaxial contactless slipring. The circuit of primary and secondary can be placed on top of ferrite, it doesn't take up any extra space.

The general overview of the WPT system is shown in Figure 8. From Figure 8 it can be seen that in a through-hole contactless slipring with coaxial layout, the primary side encircles the secondary side fully, which results in a system with a fixed air gap and asymmetrical primary and secondary. According to the design results, a prototype system is built, as shown in Figure 9. In the system, the core support frame is produced by 3D printing and the 0.1mm×500 stranded litz wire is utilized to wind the coil. The primary coil and core remain stationary, which are fed by the constant current inverter for stable power supply, and the secondary side (including secondary coil, rectifier and filtering capacitor) is combined with rotating load by the coupling device.

It can be seen that the dimension of system (include circuit) is limited to $\phi 148\text{mm} \times 48\text{mm}$ and the weight is 1.35kg, which meets the space application requirement.

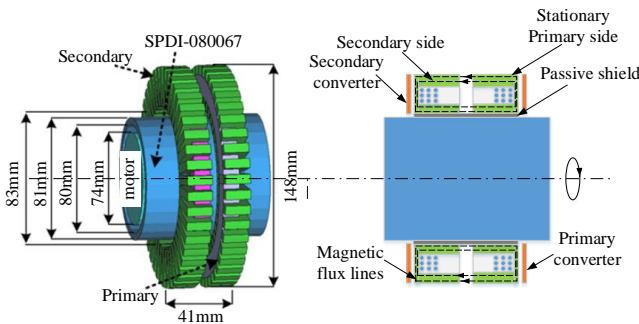


Fig 8 General overview of the WPT system

In order to verify the correctness of system design, an experimental study on output power and transmission efficiency under different loads is carried out. As is shown in Figure 10, the output power and efficiency are measured when the load current is 10A, the results show

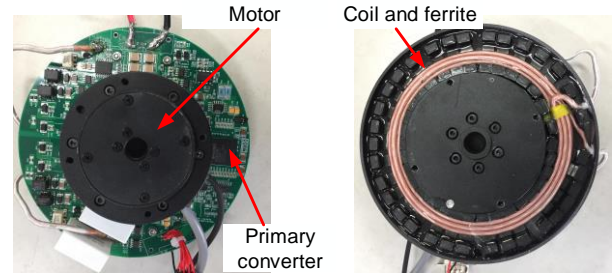


Fig 9 Core and windings of the WPT system

that the efficiency is almost constant with little fluctuation. It is proved that the proposed rotary magnetic coupler is characterized by high coupling capability, high power output stability and high efficiency.

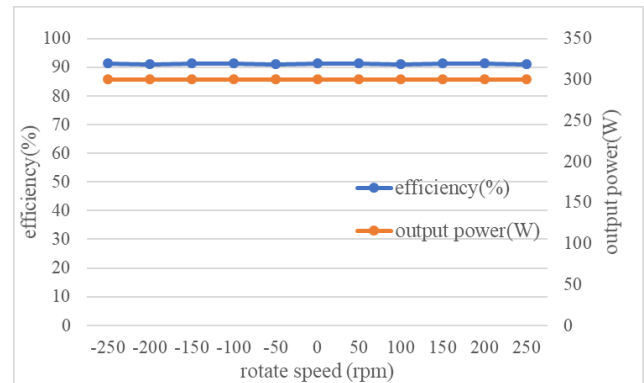


Fig 10 Output power and efficiency under rotate speed

4. CONCLUSIONS

A novel magnetic coupler of the WPT system for the space application is designed in this paper. The proposed coil enables the magnetic field to be concentrated in the coupler, which ensures strong coupling capability and thus achieves stable and efficient power transmission under rotating condition. Further, the circuit is proposed to reduce the complexity and dimension and weight of the whole system. The dimension and the weight are limited within the $\phi 148\text{mm} \times 48\text{mm}$ and the weight is 1.35kg respectively. The experimental results show that the system achieves 280W power transmission with 91.7% at 3mm air gap.

REFERENCE

[1]Ki Young Kim.Wireless power transfer principles and engineering[M].Croatia:InTech,2012:35-68.
 [2]H.Chen,A.P.Hu,D.Budgett.Power loss analysis of a TET system for high power implantable devices[C].Industrial Elec-tronics and Applications, Harbin,China,2007.
 [3]Jesús Sallá,Juan L.Villa,José Fco.Sanz.Optimal design of ICPT systems applied to electric vehicle battery charge[J].IEEE Trans on Industrial Electronics , 2009,56(6):2140-2149.